Chemistry & Biology
Article

The Biosynthesis of Teicoplanin-Type Glycopeptide Antibiotics: Assignment of P450 Mono-Oxygenases to Side Chain Cyclizations of Glycopeptide A47934

Bianka Hadatsch,[1,3] Diane Butz,[2,3] Timo Schmiederer,[2] Julia Steudle,[1] Wolfgang Wohlleben,[1] Roderich Süssmuth,[2,*] and Evi Stegmann[1,*]
[1]Institut für Mikrobiologie/Biotechnologie, Eberhard-Karls-Universität Tübingen, Auf der Morgenstelle 28, 72076 Tübingen, Germany
[2]Institut für Chemie, FG Organische Chemie, Technische Universität Berlin, Strasse des 17. Juni 124, 10623 Berlin, Germany
[3]These authors contributed equally to this work.
*Correspondence: suessmuth@chem.tu-berlin.de (R.S.), evi.stegmann@biotech.uni-tuebingen.de (E.S.)
DOI 10.1016/j.chembiol.2007.08.014

SUMMARY

Streptomyces toyocaensis **produces A47934, a teicoplanin-like type-IV glycopeptide with antibiotic activity against methicillin-resistant** ***Staphylococcus aureus*****. A47934 differs from the type-I vancomycin glycopeptides, which possess a tricyclic peptide backbone, by the presence of an additional ring closure between the aromatic amino acids 1 and 3. To elucidate the order of crosslinking reactions, P450 mono-oxygenase-inactivation mutants (Δ*staF*, Δ*staG*, Δ*staH*, and Δ*staJ*) of the A47934 producer were generated, and the accumulated intermediates were analyzed. Thus, the formation of each crosslink could unambiguously be assigned to a specific oxygenase. The structure of the released intermediates from the wild-type non-ribosomal peptide synthetase assembly line facilitated the determination of the cyclization order. Unexpectedly, the additional ring closure in A47934, catalyzed by StaG, is the second oxygenase reaction.**

INTRODUCTION

Since the discovery of vancomycin, produced by *Amycolatopsis orientalis*, in the 1950s the family of glycopeptide antibiotics has grown to several hundred currently known members [1]. Two representatives, vancomycin (**1**) and teicoplanin (**3**) (Figure 1), have been approved for clinical use and are indispensable as last-resort antibiotics against severe infections with Gram-positive bacteria, such as Enterococci and methicillin-resistant *Staphylococcus aureus* (MRSA) strains. The basis for antibacterial activity of glycopeptide antibiotics is the noncovalent binding via five hydrogen bonds from the peptidic backbone to the D-alanyl-D-alanine peptidyl residues of cell wall intermediates [2]. Thus, glycopeptide antibiotics are substrate binders that shield the substrate from transpeptidation steps in peptidoglycan assembly. However, over the past 15 years, a considerable number of glycopeptide-resistant bacteria have emerged. Current efforts to counteract these resistant strains include the exploration of natural and synthetic sources because of their potential for producing future antibacterials. An alternative approach is to rely on an established core structure and to modulate this structure by synthetic, semisynthetic, or biotechnological approaches (e.g., genetic engineering and combinatorial biosynthesis [3]). A prerequisite to the application of the latter is the understanding of the biosynthetic assembly of glycopeptide antibiotics.

The common structural feature in all glycopeptide antibiotics is the heptapeptide backbone with aromatic amino acids oxidatively coupled in the side chains via biaryl or biarylether bridges (Figure 1). They force the peptide backbone into a rigid conformation and thus confer the primary antibiotic activity of this compound class. Linear and various other monocyclic or bicyclic intermediates have been found to have no antibacterial activity [4–8]. Further structural modifications of the heptapeptide aglycon backbone consist of *N*-methylation, halogenation, and the attachment of sugar and/or fatty acid moieties.

The biosynthetic assembly of these complex structures may be considered to be tripartite, i.e., the supply of building blocks (unusual amino acids and carbohydrates), the nonribosomal peptide synthetase (NRPS) assembly line, and the modification reactions (e.g., glycosylation, methylation) [9, 10]. Previous gene-inactivation studies on the vancomycin-type (type-I) glycopeptide antibiotic balhimycin (**2**) have shown that three P450-dependent mono-oxygenases, OxyA, OxyB, and OxyC (Figure 2), are responsible for forming the three crosslinks between the aromatic amino acid side chains [5, 6]. These are performed in the following sequence: amino acids 4 and 6 (C-*O*-D ring), amino acids 2 and 4 (D-*O*-E ring), and amino acids 5 and 7 (AB ring) [5–7]. Furthermore, it has been suggested that these crosslinking reactions occur on an NRPS-oxygenase complex [11, 12].

A characteristic feature of teicoplanin-type (type-IV) glycopeptide antibiotics is an additional side chain crosslink between aromatic amino acids 1 and 3 (F-*O*-G ring) [13].

 ©2007 Elsevier Ltd All rights reserved

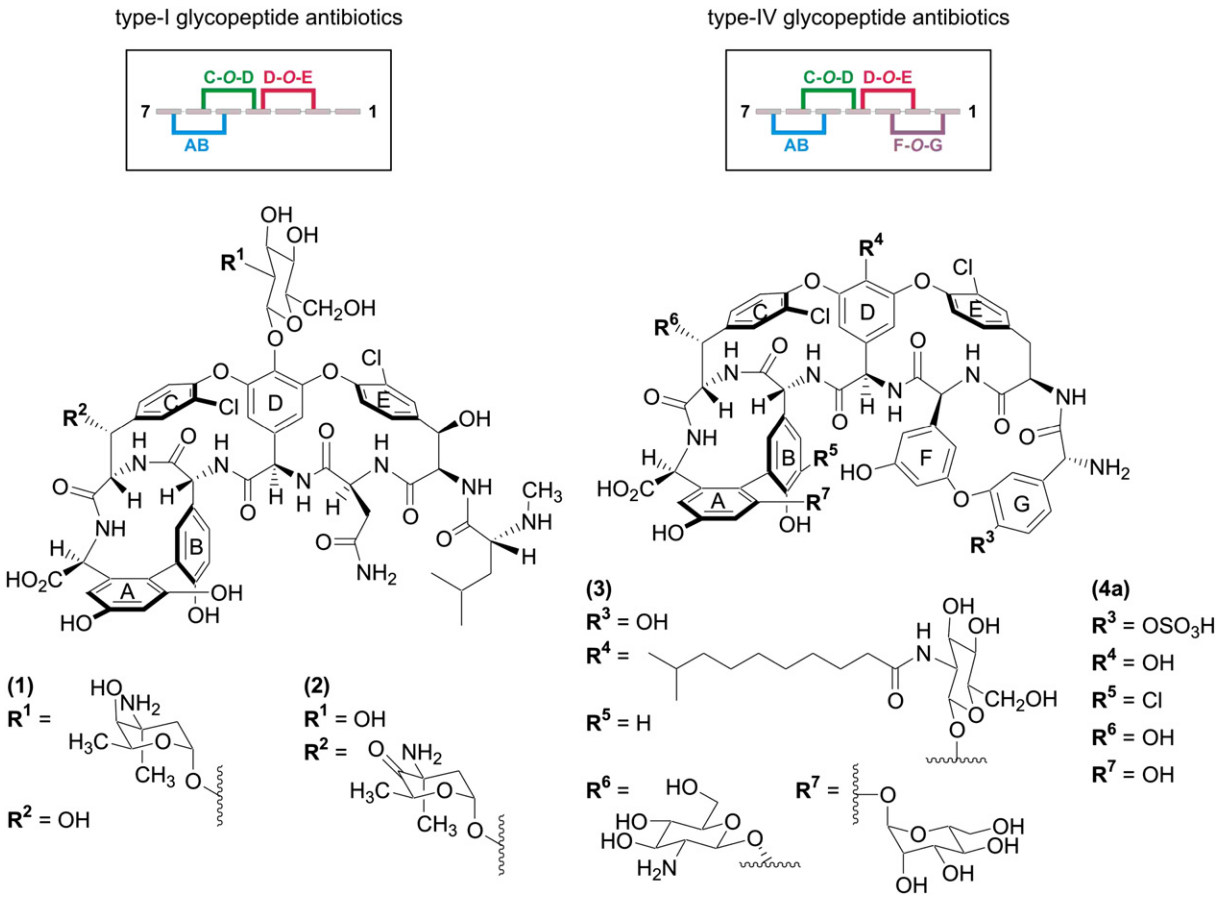

Figure 1. Structures of the Type-I Glycopeptide Antibiotics Vancomycin, 1, and Balhimycin, 2, and of the Type-IV Glycopeptide Antibiotics Teicoplanin, 3, and A47934, 4a

Framed sketches on the top reflect the structures of the peptide backbones with three and four rings (C-*O*-D, D-*O*-E, AB, and F-*O*-G), respectively.

Considering the results obtained for the vancomycin-type (type-I) glycopeptide system, this raises the question as to whether or not an analogy exists between both systems in the sequence of ring-formation reactions. We chose A47934 (**4a**), produced by *Streptomyces toyocaensis* NRRL 15009, as a model compound for type-IV glycopeptides [14]. The A47934 biosynthetic gene cluster includes four genes (*staF*, *staG*, *staH*, and *staJ*) (Figure 2) whose gene products show high sequence similarities to P450 mono-oxygenases. Analogous to the balhimycin model, they have been predicted to catalyze the four ring closures in the aromatic amino acids [15–17].

Here, we report the construction of nonpolar mutants in each A47934 oxygenase gene and the structural characterization of the synthesized intermediates by mass spectrometry. Constructed mutants were homologously and heterologously complemented by using the oxygenase genes from the A47934 producer and the oxygenase genes from the vancomycin producer, respectively. Finally, peptides related to A47934 assembly were directly identified in culture filtrates of the wild-type strain by HPLC-ESI-MS. From these studies, we were able to assign the function of the above-mentioned four P450 mono-oxygenases to distinct biosynthetic steps in A47934 assembly and were able to suggest a likely sequence of oxidative crosslinking reactions.

RESULTS

Inactivation of the Oxygenase Genes *staF*, *staG*, *staH*, and *staJ* in *Streptomyces toyocaensis*

The balhimycin biosynthetic gene cluster contains three contiguous oxygenase genes that were functionally assigned to the three side chain crosslinks of the balhimycin molecule (Figure 1). Furthermore, a stepwise sequence of the oxygenase reactions was found in the following order: OxyB → OxyA → OxyC [6]. In contrast to type-I glycopeptides, the glycopeptide antibiotic A47934 possesses four side chain crosslinks. Accordingly, from sequence analyses of the A47934-producer strain, four genes (*staF*, *staG*, *staH*, and *staJ*) were identified and predicted to be responsible for the four oxidative couplings during biosynthesis. Phylogenetic analysis of P450 mono-oxygenases of the balhimycin A47934 and other glycopeptide producers showed pronounced sequential relationships,

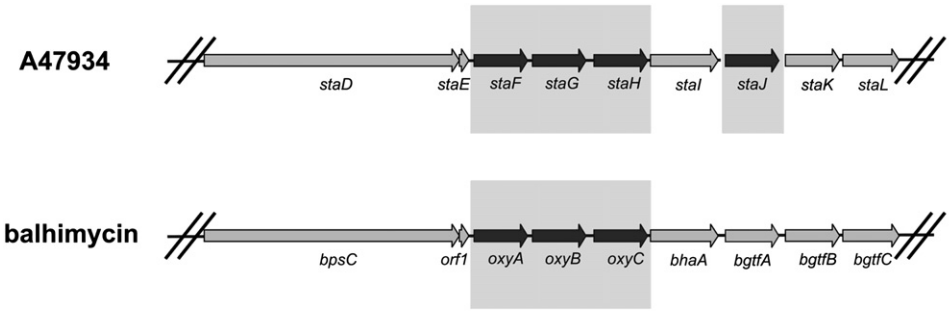

A47934

gene	function/homology
staD	peptide synthetase
staE	mbtH-like protein
staF	P450 monooxygenase
staG	P450 monooxygenase
staH	P450 monooxygenase
staI	$FADH_2$-dependent halogenase
staJ	P450 monooxygenase
staK	$FADH_2$-dependent halogenase
staL	sulfotransferase

balhimycin

gene	function/homology
bpsC	peptide synthetase
orf1	mbtH-like protein
oxyA	P450 monooxygenase
oxyB	P450 monooxygenase
oxyC	P450 monooxygenase
bhaA	$FADH_2$-dependent halogenase
bgtfA	glycosyltransferase
bgtfB	glycosyltransferase
bgtfC	glycosyltransferase

Figure 2. Genetic Organization of the Oxygenase Genes in the A47934 and Balhimycin Biosynthetic Gene Cluster

as shown in Figure 3. Subsequently, from these relationships and the knowledge of balhimycin aglycon assembly, distinct biosynthetic steps were deduced for the P450 mono-oxygenases. As a consequence, StaF (72% identical to OxyA, but no more than 39% identical to the other Oxy proteins) was predicted to be involved in the crosslinking of amino acids 2 and 4 (D-*O*-E ring), StaH (77% identical to OxyB, but no more than 49% identical to the other Oxy proteins) was predicted to be involved in the crosslinking of amino acids 4 and 6 (C-*O*-D ring), and StaJ (68% identical to OxyC, but no more than 50% identical to the other Oxy proteins) was predicted to be involved in the crosslinking of amino acids 5 and 7 (AB ring). Only StaG shows no significant identity to any of the balhimycin oxygenases (no more than 44%); therefore, it was hypothesized to catalyze the teicoplanin-specific crosslink between amino acids 1 and 3 (F-*O*-G ring).

In-frame deletion mutants of all oxygenase genes were constructed to functionally assign the four oxygenases, StaF, StaG, StaH, and StaJ, to distinct biosynthetic steps. The nonreplicative gene-inactivation plasmids, pBHstaF, pBHstaG, pBHstaH, and pBHstaJ (for construction, see Experimental Procedures), carrying the flanking regions of the corresponding oxygenase gene were used for transformation of the wild-type strain *S. toyocaensis* by protoplast transformation. The selection was based on the plasmid apramycin resistance marker and therefore only those recombinants that had integrated the inactivation plasmids pBHstaF, pBHstaG, pBHstaH, or pBHstaJ into the chromosome via homologous recombination between one of the cloned fragments and the corresponding chromosomal gene region were able to grow. The presence of the plasmids was verified by PCR amplification of a fragment of the apramycin-resistance cassette (data not shown). In order to select gene deletion mutants in which a second homologous recombination event via the second cloned fragment had occurred, the inactivation mutants were subjected to a ''stress'' treatment (see Experimental Procedures). This protocol has been developed to increase the probability of a second crossover event. After the application of this ''stress'' protocol, 900, 600, 5000, and 900 colonies for mutations in *staF*, *staG*, *staH*, and *staJ*, respectively, were examined on R5 plates with and without apramycin. For *staF* 15, for *staG* 14, for *staH* 32 and for *staJ* eight colonies were identified which had lost the plasmid as indicated by the lack of the apramycin resistance. Subsequent PCR analyses confirmed the internal deletion of the oxygenase genes (Figure 4). As a result of this selection process, 6 Δ*staF*, 1 Δ*staG*, 13 Δ*staH*, and 1 Δ*staJ* mutant were identified as in-frame deletion mutants. The *B. subtilis* bioassay showed that these colonies were incapable of producing A47934 (data not shown), confirming that, in those cases, the second crossover had led to the exchange of the wild-type allele for the deleted oxygenase genes, and not to the reversion of clones to the wild-type.

Analyses of the Metabolite Spectrum of the Deletion Mutants via HPLC-ESI-MS and -MS/MS

Based on previous studies of the balhimycin system [5, 6], the chlorination of peptide metabolites was employed as a suitable indicator for mass spectrometric detection of glycopeptide metabolites (Figures 5 and 6). Culture filtrates of the wild-type that have been used as a reference showed A47934 (M = 1311.1 Da) (**4a**) and the nonsulfated analog (M = 1231.2 Da) (**4b**) as the main metabolites. The

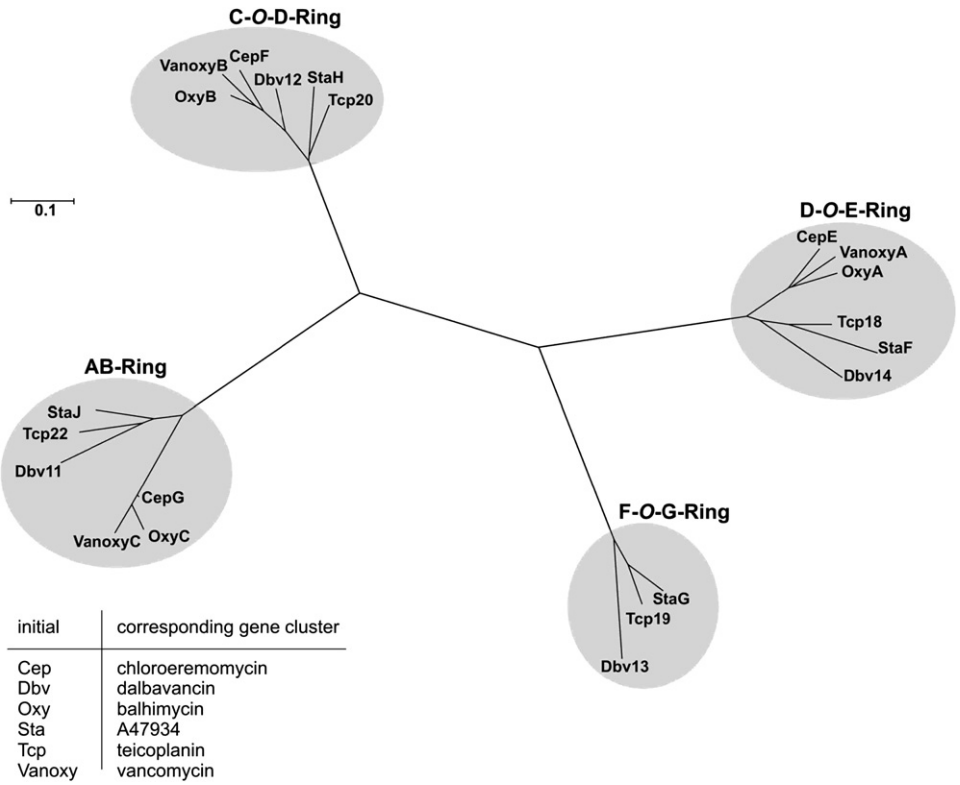

Figure 3. Phylogenetic Analyses of Oxygenase Proteins from Vancomycin-Type and Teicoplanin-Type Glycopeptides
Oxygenases with significant homologies are assigned to putative functions: the cyclization of the C-*O*-D, D-*O*-E, F-*O*-G, and AB rings.

HPLC-ESI-MS analyses of all four oxygenase deletion mutants indicated the absence of A47934 detected in the culture filtrates of the *S. toyocaensis* wild-type. The structural assignment of peptides from Δ*staF*, Δ*staG*, Δ*staH*, and Δ*staJ* mutants had to be performed solely based on MS/MS experiments since an isolation of milligram amounts (e.g., for NMR experiments) was not possible due to a very low titer.

The Δ*staJ* mutant produces only the tricyclic hexa- (**9a**, **9b**) and heptapeptides (**16a**, **16b**) (Figure 5), and the interpretation of fragment spectra indicates the presence of structures with C-*O*-D, F-*O*-G, and D-*O*-E rings. This implies that StaJ catalyzes the AB ring formation. In the balhimycin system, the AB ring is the third, and concomitantly the final, ring formed by OxyC. The sequential analogy of StaJ and OxyC on a phylogenetic base (Figure 3) supports the functional assignment deduced from the experimental findings.

For the Δ*staF* mutant, five metabolites were identified (Figures 5 and 6). In addition to the main metabolite on the hexapeptide level, a hexapeptide with two side chain cyclizations (C-*O*-D and F-*O*-G ring) (**8b**), a monocyclic hexapeptide (C-*O*-D) (**6b**), and a linear hexapeptide (**5b**) were detected. On the heptapeptide level, we observed two main metabolites with molecular masses corresponding to a bicyclic (**13b**) and a tricyclic heptapeptide (**15b**). The interpretation of the fragment spectra localized the side chain cyclizations at the C-*O*-D/F-*O*-G and C-*O*-D/F-*O*-G/AB rings, respectively. The absence of the D-*O*-E ring in Δ*staF* mutant intermediates indicates that StaF is responsible for D-*O*-E ring formation. In the balhimycin producer, D-*O*-E ring formation is catalyzed by OxyA as the second step of the oxygenase reactions, which supports the validity of the assumption based on the sequence analysis of OxyA and StaF (Figure 3). Remarkably, StaJ is able to catalyze the AB cyclization on the heptapeptide level regardless of the presence of the D-*O*-E ring, which differs from the sequential ring assembly in the balhimycin system.

In the culture filtrate of the Δ*staG* mutant, molecular masses that correlate to a monocyclic hexapeptide with the C-*O*-D ring (**6b**) and a bicyclic heptapeptide (**12b**) with C-*O*-D and AB crosslinks as main metabolites were identified. The molecular masses of a linear (**5b**) and a bicyclic hexapeptide (C-*O*-D/D-*O*-E) (**7b**) as well as of a monocyclic (C-*O*-D) (**11b**) and a tricyclic heptapeptide (**14b**) were detected, albeit in much lower concentrations. Since **14b** occurred only in traces, the crosslinking pattern could not be unambiguously determined. However, the retention time differs from other tricyclic heptapeptides, **15b** of Δ*staF* (C-*O*-D, F-*O*-G, and AB) and **16b** of Δ*staJ* (C-*O*-D, F-*O*-G, and D-*O*-E), which argues for the C-*O*-D/D-*O*-E/AB ring combination as the only remaining possibility. These data suggest that StaG is the mono-oxygenase forming the F-*O*-G ring. This finding is supported by sequence analysis (Figure 3) which indicates a significant

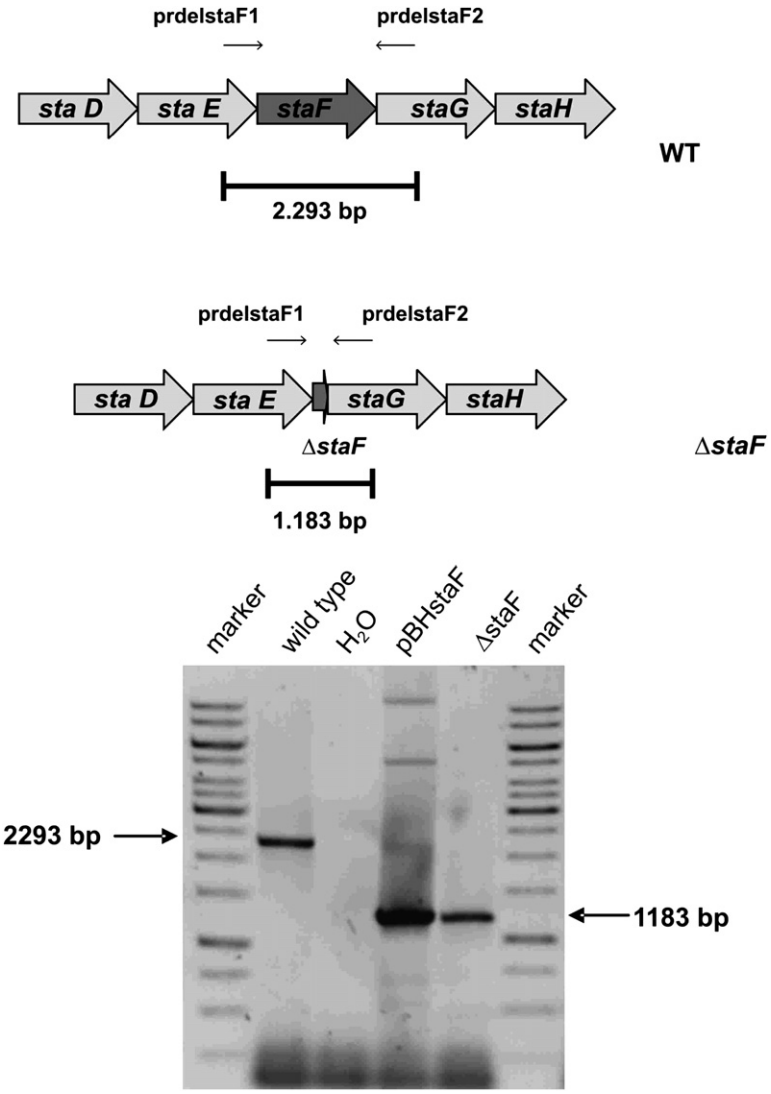

Figure 4. PCR Analysis for Verification of the In-Frame Mutation in *staF*

The in-frame mutation is representative of all of the Δ*sta* mutants. Marker, 1 kb ladder; lane 1, 2293 bp *staF* fragment with *S. toyocaensis* wild-type DNA as template; lane 2, negative control with $H_2O_{deion.}$ as template; lane 3, 1183 bp fragment with plasmid pBHstaF as template; lane 4, 1183 bp fragment with *S. toyocaensis ΔstaF* DNA as template. In all cases, the primer pair prdelstaF1/F2 (arrows; for the sequence, see Table S2) was used.

lack of similarity to other mono-oxygenases of the vancomycin system. Furthermore, the results suggest that F-*O*-G ring formation is not a precondition for the ring formation catalyzed by StaF, and that StaJ can catalyze AB ring formation regardless of the cyclization pattern of the molecule (as observed in the Δ*staF* mutant).

Analysis of the Δ*staH* mutant revealed a molecular mass of 1239.4 Da (**10b**) and a mass shift of 8 atomic mass units (amu) to higher masses, compared to the nonsulfated wild-type metabolite (**4b**). This lack of all four side chain cyclizations corresponds to a linear heptapeptide structure that was confirmed by MS/MS fragment spectra. An additional metabolite of Δ*staH* with a molecular mass of 1074.2 Da (**5b**) suggests a linear, nonsulfated, C-terminally truncated hexapeptide. These findings confirm that StaH catalyzes the first ring closure reaction of the peptide cyclization sequence. This biosynthetic step is analogous to the first oxygenase reaction (C-*O*-D) in the balhimycin biosynthesis, which is catalyzed by OxyB.

Identification of Biosynthetic Intermediates in Culture Filtrates of the Wild-Type Strain *Streptomyces toyocaensis* via HPLC-ESI-MS and -MS/MS

In order to reveal information about the teicoplanin-type glycopeptide biosynthesis, an alternative approach that was independent of gene-inactivation experiments was persued. Hence, culture filtrates of the A47934 wild-type producer were screened for biosynthetic intermediates. We predominantly used the characteristic isotope pattern of chlorinated di- to heptapeptides as a marker for the identification of these putative A47934 biosynthesis intermediates. Furthermore, we considered tailoring reactions, (e.g., sulfatation and oxidative side chain cyclization) to be variables occurring at various points in time during or after peptide assembly. HPLC-ESI-MS analyses were performed as full-scan experiments that were searched by the extracted ion chromatogram (EIC) mode for putative *m/z* values. As a result of this screening, molecular

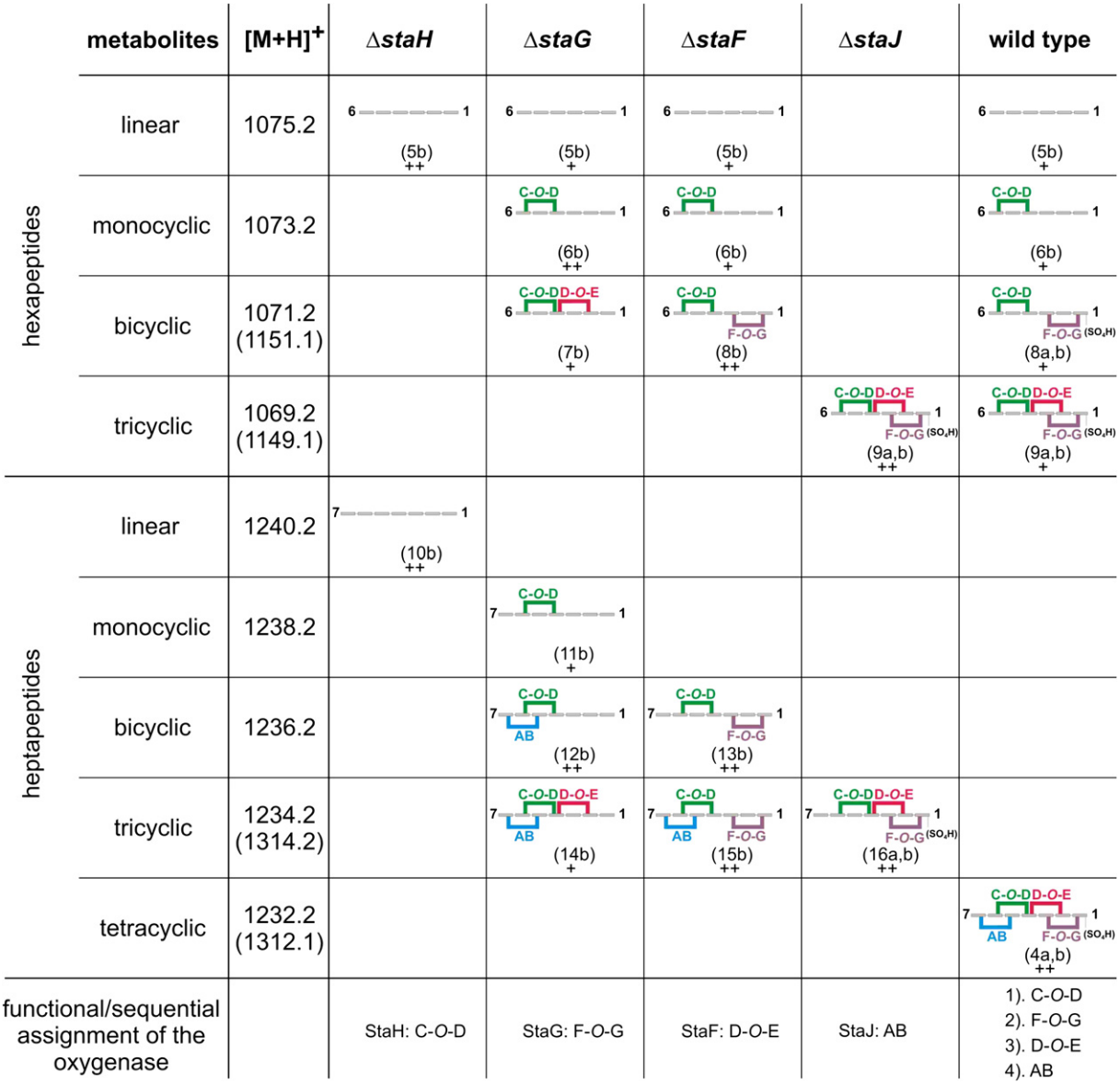

Figure 5. Synopsis of all Hexa- and Heptapeptides Detected in the Culture Filtrates of A47934 Mutants—Δ*staH*, Δ*staG*, Δ*staF* and Δ*staJ*—and Wild-Type Characterized by HPLC-ESI-MS and -MS/MS

All metabolites are fully chlorinated. A semiquantitative estimation of metabolite synthesis was performed according to ionization yields (++ = main metabolite; + = minor metabolite, < 10% total production). Metabolites designated with "a" are sulfated; those designated with "b" are nonsulfated ($[M+H]^+$ in brackets). $[M+H]^+$ values have been calculated from the molecular formula.

masses of C-terminally truncated peptides corresponding to hypothetically calculated di-, tri-, tetra-, penta-, hexa-, and heptapeptides were detected. A more detailed and specific analysis with HPLC-ESI-MS/MS daughter ion scans yielded characteristic fragment spectra, which were assigned to the peptides related to A47934. The interpretation of analytic data by using a combination of molecular masses and fragment spectra resulted in a set of compounds depicted in Figure 5 (dipeptides-pentapeptides data not shown).

Out of these compounds, the dipeptides to pentapeptides are all linear. Among the hexapeptides, four derivatives, corresponding to different degrees of cyclization, were detected. Interpretation of daughter ion experiments revealed a linear hexapeptide (**5b**), a monocyclic hexapeptide (**6b**) with a C-*O*-D ring, and a bicyclic hexapeptide (**8a**, **8b**) with C-*O*-D and F-*O*-G rings. Based on the fragment spectra of the tricyclic hexapeptide (**9a**, **9b**), there remains only one possibility for the assignment of the structures with the C-*O*-D, F-*O*-G, and D-*O*-E rings. On the heptapeptide level, only the tetracyclic peptides were observed (**4a**, **4b**). With regard to sulfation, only the bi- and tricyclic hexapeptides and the tetracyclic heptapeptide were found to have been modified.

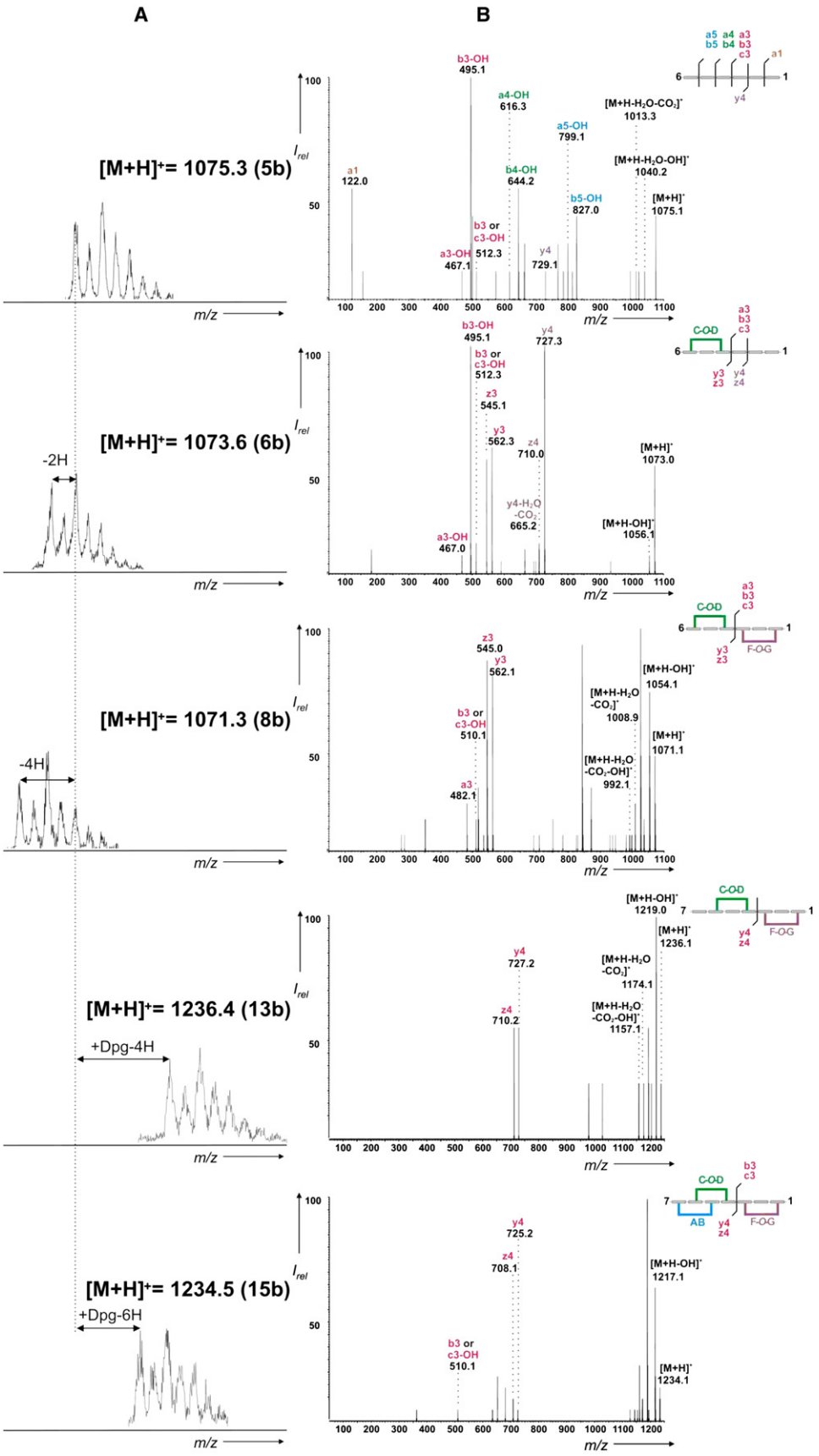
A
B
[M+H]+= 1075.3 (5b)
[M+H]+= 1073.6 (6b)
-2H
[M+H]+= 1071.3 (8b)
-4H
[M+H]+= 1236.4 (13b)
+Dpg-4H
[M+H]+= 1234.5 (15b)
+Dpg-6H
m/z
Irel
b3-OH 495.1
a4-OH 616.3
a5-OH 799.1
[M+H-H2O-CO2]+ 1013.3
[M+H-H2O-OH]+ 1040.2
a1 122.0
b4-OH 644.2
b5-OH 827.0
[M+H]+ 1075.1
b3 or c3-OH 512.3
a3-OH 467.1
y4 729.1
y4 727.3
z3 545.1
y3 562.3
z4 710.0
y4-H2O -CO2 665.2
[M+H-OH]+ 1056.1
[M+H]+ 1073.0
a3-OH 467.0
z3 545.0
y3 562.1
[M+H-H2O -CO2]+ 1008.9
[M+H-OH]+ 1054.1
[M+H]+ 1071.1
b3 or c3-OH 510.1
[M+H-H2O -CO2-OH]+ 992.1
a3 482.1
[M+H-OH]+ 1219.0
[M+H]+ 1236.1
y4 727.2
z4 710.2
[M+H-H2O -CO2]+ 1174.1
[M+H-H2O -CO2-OH]+ 1157.1
y4 725.2
z4 708.1
[M+H-OH]+ 1217.1
[M+H]+ 1234.1
b3 or c3-OH 510.1
C-OD
F-OG
AB

Complementation of the Deletion Mutants Δ*staF*, Δ*staG*, Δ*staH*, and Δ*staJ* with the A47934 and the Corresponding Vancomycin Oxygenases

Complementation experiments were performed to exclude the polar effects of the genetic manipulations in the oxygenase mutants Δ*staF*, Δ*staG*, Δ*staH*, and Δ*staJ*. We could show, via agar diffusion assays for antibacterial activity (data not shown) and HPLC-ESI-MS, that the insertion of the respective plasmids, pSETstaF, pSETstaG, pSETstaH, and pSETstaJ (containing the A47934 oxygenase genes under the control of the constitutive promoter *PermE*), at the ΦC31 attachment site (*attB*) could fully complement the mutants and thus reconstitute A47934 synthesis.

Crosscomplementation experiments were performed to confirm the functional relationship between A47934 oxygenase genes and the corresponding genes from producers of vancomycin-like glycopeptides that was deduced from in situ sequence analysis (Figure 3). Because of the predicted functional equivalence between the balhimycin and the vancomycin oxygenases and because of the availability of the expression plasmids pSETvanoxyA, pSETvanoxyB, and pSETvanoxyC [7] containing the vancomycin oxygenase genes, which are under the control of the constitutive promoter *PermE*, we used them for crosscomplementation experiments. As predicted, we were able to complement the Δ*staH* mutant with only the corresponding *vanoxyB* gene, and the Δ*staJ* mutant with only the corresponding *vanoxyC* gene. In both cases, the production of active A47934 was restored. Although VanoxyA shows the highest identity to StaF, no complementation was achieved, nor was complementation possible with the other vancomycin oxygenase genes. StaG is unique because it shows no significant identity to any of the balhimycin, or rather vancomycin, oxygenase genes. As expected, no complementation of the Δ*staG* mutant was possible.

DISCUSSION

In recent studies, the side chain crosslinking reactions performed by P450-type mono-oxygenases were extensively investigated to determine the biosynthesis of the vancomycin-type glycopeptide balhimycin. Each of the three balhimycin oxygenase genes (*oxyA–C*), identified in the balhimycin biosynthesis gene cluster, is correlated to one of the three side chain cyclizations, for which a strict sequence has been determined (OxyB → OxyA → OxyC) [6]. Analogous to this approach, we utilized this gene-inactivation strategy to gain insights into the oxygenase reactions of the four-fold, side chain-cyclized teicoplanin-type glycopeptide A47934. The previously proposed oxygenase genes for the aglycon assembly of A47934 *staF*, *staG*, *staH*, and *staJ* [15] were inactivated by the generation of deletion mutants. The subsequent HPLC-ESI-MS analysis of culture filtrates of these mutants (Δ*staF*, Δ*staG*, Δ*staH*, and Δ*staJ*) revealed peptides with different degrees of cyclization (Figure 5). The location of the rings in the peptide backbones of mutant metabolites was determined via the assignment of fragments from MS/MS experiments. From the mass spectrometric data obtained for all mutants, we can deduce and assign enzyme functions to each of the four P450-type monooxygenases: StaF, StaG, StaH, and StaJ.

From the Δ*staH* mutant, only linear metabolites (**5b**, **10b**) were detected. Based on the findings from the balhimycin model [11], StaH would perform the first ring-closure reaction, which involves the C-*O*-D ring. This is in full accordance with the similarity of OxyB and StaH based on phylogenetic data. Furthermore, the mass spectrometric analyses imply that the subsequent action of other oxygenases is blocked if the first ring closure has not been catalyzed, since no other cyclic derivatives were found.

In the cultural filtrates of the Δ*staJ* mutant, only the tricyclic peptides (**9a**, **9b** and **16a**, **16b**) were detected. Because mass spectrometric data only showed the C-*O*-D, F-*O*-G, and D-*O*-E rings, we can clearly assume that StaJ oxygenase catalyzes AB ring formation. The finding of the tricyclic heptapeptide (**15b**), synthesized by the Δ*staF* mutant, with C-*O*-D, F-*O*-G, and AB rings assigns StaF to D-*O*-E ring formation. The fact that, in addition to **15b**, significant amounts of metabolites **5b**, **6b**, **8b**, and **13b** were detected, however, leads to further assumptions about ring formation by oxygenases of the A47934 biosynthesis gene cluster. For example, StaJ can catalyze AB ring formation even if the D-*O*-E-ring synthesized by StaF is missing.

The Δ*staG* mutant predominantly synthesizes a monocyclic (C-*O*-D) hexapeptide (**6b**) and a bicyclic (C-O-D, AB) heptapeptide (**12b**). In accordance with the abovementioned finding for the Δ*staF* mutant, this shows that StaJ can also act on a monocyclic heptapeptide to catalyze AB ring formation. Furthermore, some minor metabolites, in particular (**14b**) a tricyclic heptapeptide, were detected, which suggests that StaG is responsible for the F-*O*-G ring. Together with the results obtained for the Δ*staF* mutant, these data show that StaJ can catalyze the formation of the AB ring on the heptapeptide level, regardless of the cyclization status of the other amino acid residues, if the C-*O*-D ring is present. As previously mentioned, the results from the gene-inactivation experiments suggest that StaH catalyzes the first ring closure (C-*O*-D)

Figure 6. Representative Mass Spectrometric Analysis of Metabolites Detected in the Culture Filtrates of the Δ*staF* Mutant

(A) Experimentally determined molecular masses and characteristic isotope patterns of metabolites. Mass shifts indicate structural differences between the compounds.

(B) Assignment of fragment spectra from MS/MS experiments to various peptide structures. (The designation of the fragment ions arising from cleavage sites along the peptide backbone is in accordance with the nomenclature of Roepstorff and Fohlman [29]. Secondary fragmentation events occurring at phenolic hydroxy groups lead to $[M+H-OH]^+$ and the corresponding fragment ions $[F-OH]^+$.)

but, subsequent conclusions about a biosynthetic sequence are less obvious. StaG catalyzes the F-*O*-G cyclization step; however, if StaG is nonfunctional, D-*O*-E ring formation (catalyzed by StaF) can still occur. Finally, StaJ catalyzes the cyclization (AB) on the heptapeptide backbone. Further confirmation of the assignment of oxygenase functions came from complementation experiments. All oxygenase genes could be homologously complemented by the respective Sta oxygenase gene, and thus formation of A47934 production could be restored. In addition, crosscomplementation experiments were performed with P450 mono-oxygenases, from type-I glycopeptide producers, based on the sequential similarity of oxygenases in the vancomycin producer. Remarkably, a successful complementation was achieved for the Δ*staH* mutant with the most similar oxygenase, *vanoxyB* (C-*O*-D), and for the Δ*staJ* mutant with *vanoxyC* (AB). No functional reconstitution was obtained upon complementation of the Δ*staF* mutant with *vanoxyA*, although both proteins have an identity of 69% and the functionality of the complementation construct containing the *vanoxyA* gene has already been shown [7]. Because Δ*staF* catalyzes the formation of the F-*O*-G ring, which is absent in vancomycin-type glycopeptides, VanoxyA might not be capable of recognizing F-*O*-G ring-containing peptides as substrates. Despite a considerable sequential homology between StaF and VanoxyA, the action of VanoxyA may be too specific for the recognition of peptide intermediates from A47934. In contrast, the substrates of OxyC and StaJ also differ in the presence of the F-*O*-G ring, which does not affect the functional equivalence of these enzymes.

Although we were able to assign oxygenase functions to distinct catalytic reactions, based on gene inactivation experiments, no unambiguous sequence for the oxidative steps could be deduced. The findings for the oxygenases of the A47934 biosynthetic gene cluster of *S. toyocaensis* rather imply a skipping of some of the oxidative biosynthetic steps, as found for bicyclic and tricyclic peptides synthesized by Δ*staG* and Δ*staF*. Therefore, we speculated that this substrate flexibility of the oxygenases may also exist in the wild-type. In order to clarify whether a preferred sequence in side chain crosslinking exists or whether a randomized action of StaF and StaJ occurs, a second complementary approach was explored.

Previous observations, by other groups [18, 19], have shown that biosynthetic intermediates found in minute amounts in culture filtrates of wild-type antibiotic producers can give insight into the biosynthesis of natural products. We transferred this approach to peptide metabolites of the glycopeptide type. In wild-type fermentations of *S. toyocaensis*, various peptide intermediates that have been assigned to A47934 biosynthesis were detected (Figure 5). The detected di- to pentapeptides are all linear (data not shown), which suggests that the first oxidative crosslink performed by StaH occurs at the hexapeptide stage. With the exception of the tetracyclic heptapeptide aglycon (**4a**, **4b**), all other detected peptides in wild-type fermentations were hexapeptides. Among the four hexapeptide derivatives, the complete set was found ranging from a linear (**5b**), to a monocyclic (**6b**), to a bicyclic (**8a**, **8b**), and to a tricyclic (**9a**, **9b)** derivative. These derivatives were of defined structure (i.e., only one ring-closure pattern was detected, and derivatives displaying alternative ring structures were not found). In contrast to the skipping or randomization of crosslinking steps, observed for the gene-inactivation mutants Δ*staG* and Δ*staF*, the results from the analysis of wild-type cultures suggest that there is a preferred sequence for oxidative ring-closure reactions. This sequence is as follows: C-*O*-D ring → F-*O*-G ring → D-*O*-E ring → AB ring, where StaH, StaG, StaF, and StaJ are the corresponding catalysts. While the results obtained for the wild-type indicate a defined sequence, the intermediates in the culture filtrates of the deletion mutants indicate oxygenase reactions of lowered specificity. Obviously, StaF and StaJ represent oxygenases of decreased substrate specificity, which becomes apparent in the deletion mutants, possibly because of the accumulation of intermediates only present in the deletion mutants.

A common feature of the biosyntheses of type-I and type-IV glycopeptide antibiotics is that the ring systems are synthesized by the oxygenases at a time point not earlier than the hexapeptide stage. In both glycopeptide systems, the C-*O*-D ring is consistently the first ring to be closed, and no skipping of this reaction with subsequent oxidative steps is allowed. The second oxidative step in A47934 assembly is the formation of the F-*O*-G ring. This biosynthetic step is followed by the formation of the D-*O*-E ring and the AB ring, with both corresponding to the sequence found for the assembly of the balhimycin aglycon. This finding seems remarkable since the F-*O*-G system does not necessarily contribute to the antibiotic activity. Type-II glycopeptide (actinoidin) antibiotics with aromatic amino acids in positions 1 and 3 lack the F-*O*-G ring but still show antibiotic activity. Therefore, intuitively one would have expected that the F-*O*-G ring is the last ring formed and that it represents an ''optional,'' less-controlled step.

In summary, the oxidative crosslink assembly found in the balhimycin system [6] is also observed in the A47934 wild-type. The mass spectrometric data imply an order of the cyclization steps (StaH, then StaG, StaF, and StaJ). However, in contrast to the balhimycin system, the A47934 oxygenases exhibit flexibility if the substrate supply is modified, as observed for the A47934 oxygenase mutants Δ*staG* and Δ*staF*.

With regard to the assembly of A47934, we also assume a close interaction of NRPS and oxygenases in a protein-protein complex, as has previously been proposed [11, 12]. In this context, it has been shown with PCP-bound linear hexa- and heptapeptides of the vancomycin biosynthesis that these are suitable substrates of OxyB [12]. The presence of cyclized hexapeptides in the gene-inactivation mutants and the wild-type strain correlates with this model and extends its validity to teicoplanin-type glycopeptides.

SIGNIFICANCE

The P450-type mono-oxygenases StaF, StaG, StaH, and StaJ of the A47934-producer *S. toyocaensis* have the capacity to crosslink linear precursor peptides to form a tetracyclic antibiotic scaffold. This scaffold is not only a characteristic structural feature of glycopeptide antibiotics, but it is also the base for antibiotic activity. By means of gene inactivation, a precise correlation between the position of a biaryl- or biarylether crosslink in the peptide backbone and its catalyzing oxygenase was elaborated. Unlike with the vancomycin-type glycopeptide balhimycin, the gene-inactivation studies show a relaxed substrate specificity of the Sta oxygenases. Only the combination of the mass spectrometric analysis of both the gene-inactivation mutants and the wild-type cultures allows for a functional assignment and deduction of a biosynthetic sequence for oxygenase steps. This approach underlines the potential of HPLC-ESI-MS of wild-type cultures as a predictive tool for biosynthetic pathways, particularly for peptidic secondary metabolites, and points to the problem that investigations with putative intermediates and purified enzymes may indicate the occurrence of biosynthetic reactions that only take place under artificial conditions. This study increases the understanding of glycopeptide biosyntheses and is considered to be a representative example for type-IV glycopeptide antibiotics. Detailed knowledge of biosynthetic pathways is the prerequisite for combinatorial biosynthesis that may serve as a tool for the generation of novel antibiotics.

EXPERIMENTAL PROCEDURES

Bacterial Strains and Plasmids

Escherichia coli XL1-blue [20] was used for cloning purposes, and the methylation-deficient strain *E. coli* JM110 was used to obtain unmethylated DNA for *Streptomyces* transformations.

Streptomyces toyocaensis NRRL15009 is the A47934-producing wild-type and was used to generate the oxygenase mutants BHstaF, BHstaG, BHstaH, and BHstaJ (this study).

The inactivation plasmids pBHstaF, pBHstaG, pBHstaH, and pBHstaJ are derivatives of the nonreplicative vector pA18mob (Table S1, see the Supplemental Data available with this article online). The vector pA18mob was constructed for the generation of insertion and gene replacement plasmids. pA18mob derives from the vector pK18mob [21] and contains an *oriT* and an apramycin-resistance cassette from the plasmid pSET152 [22] instead of the kanamycin cassette.

The integrative expression vector pSETermEp* [7] was used for the complementation experiments.

Media and Culture Conditions

E. coli strains were grown in Luria broth (LB) medium [23] at 37°C and were supplemented with 100 μg ml^{-1} apramycin when necessary to maintain plasmids.

Liquid cultures of *S. toyocaensis* were cultivated in 100 ml R5 medium in an orbital shaker (180 rpm) in 500 ml Erlenmeyer flasks with steel springs at 30°C. Liquid/solid media were supplemented with 50 μg ml^{-1} apramycin to select for strains carrying integrated antibiotic-resistance genes.

Cloning, Restriction Mapping, and In Vitro Manipulation of DNA

Methods for isolation and manipulation of DNA were described by Sambrook et al. [24] and Kieser et al. [25]. PCR fragments were isolated from agarose gels with QIAquick (QIAGEN, Hilden, Germany). Restriction nucleases were purchased from various suppliers and used according to their specifications. Transformation of *E. coli* was performed by using the $CaCl_2$ method described in Sambrook et al. [24]. *E. coli* XL1-blue was used for standard cloning experiments.

Construction of the Inactivation Plasmids pBHstaF, pBHstaG, pBHstaH, and pBHstaJ

Plasmids were constructed for the in-frame deletion of the individual oxygenase genes.

All PCR protocols that were followed are included in the Supplemental Data.

For the deletion of *staF*, a 1965 bp upstream (frstaF1) and a 1954 bp downstream fragment (frstaF2) of *staF* were amplified by PCR with the primers prstaF1.1/prstaF1.2 and prstaF2.1/prstaF2.2, respectively. The frstaF1 fragment consists of part of the *staD* gene and the complete *staE* gene. The fragment frstaF2 consists of the complete *staG* gene and part of the *staH* gene. The primers are equipped with synthetic restriction sites at the 3′ and 5′ ends (EcoRI/XbaI and XbaI/HindIII). Both fragments were cloned into the vector pA18mob, resulting in the plasmid pBHstaF.

The cloning of the plasmids pBHstaG, pBHstaH, and pBHstaJ follows the same strategy as that described for the cloning of plasmid pBHstaF. The corresponding primers are equipped with the same synthetic restriction sites.

The flanking regions of *staG* were amplified by PCR with the primers prstaG1.1/prstaG1.2 and prstaG2.1/prstaG2.2, resulting in a 2010 bp fragment, which consists of part of the *staD* gene and the complete *staE* and *staF* genes, and a 2092 bp fragment, which encodes for the *staH* gene and part of the *stal* gene, respectively. The fragments were cloned into the vector pA18mob, resulting in the plasmid pBHstaG.

For the inactivation of *staH*, a 2038 bp and a 2031 bp fragment were amplified by PCR with the primers prstaH1.1/prstaH1.2 and prstaH2.1/prstaH2.2, respectively. The fragment frstaH1 consists of the complete *staG* gene and part of the *staF* gene, and frstaH2 encodes for the complete *stal* gene and part of the *staJ* gene. Both fragments were cloned into the pA18mob, resulting in the plasmid pBHstaH.

The inactivation plasmid pBHstaJ contains the flanking fragments of *staJ* with a size of 2093 bp, which consist of *stal* and part of *staH*, and a fragment of 1950 bp, which encodes *staK* and part of *staL*. The fragments were amplified by PCR with the primers prstaJ1.1/prstaJ1.2 and prstaJ2.1/prstaJ2.2, respectively.

Construction of the Complementation Plasmids pSETstaF, pSETstaG, pSETstaH, and pSETstaJ

The expression plasmids pSETstaF, pSETstaG, pSETstaH, and pSETstaJ were constructed for the complementation of the oxygenase mutants.

All PCR protocols that were followed are included in the Supplemental Data.

The primers prcostaF1/2 were used to amplify the complete *staF* gene from genomic DNA of *S. toyocaensis* with a synthetic ribosome binding site (GGAGG) typical for *Streptomyces*, and the start and stop codon of the gene, respectively. The primer prcostaF1 carries a HindIII at the 5′ end, and prcostaF2 carries an XbaI synthetic restriction site at the 3′ end. The amplified fragment of 1211 bp was cloned into the vector pSETermEp* [7], which contains the strong constitutive *PermE** promoter, resulting in the plasmid pSETstaF.

The cloning of the plasmids pSETstaH and pSETstaJ follows the same cloning strategy as for pSETstaF. For *staH* and *staJ*, 1232 and 1213 bp fragments, respectively, were amplified and cloned into pSETermEp* (Table S1).

The primers prcostaG1/2 carry a *Hin*dIII and a *Bam*HI synthetic restriction site, respectively, as well as a synthetic ribosome-binding site (5′-GGAGG-3′). The amplified fragment, consisting of the complete *staG* gene with start and stop codons, of 1190 bp was cloned into pSETermEp*, resulting in pSETstaG.

Protoplast Transformation of *S. toyocaensis*

The transformation of *S. toyocaensis* was carried out as described by Matsushima and Baltz [26]. The cells were overlayed with top agar to a final apramycin concentration ranging from 25 μg ml^{-1} to 100 μg ml^{-1}.

'Stress' Treatment for Increasing the Frequency of Crossover Events in *S. toyocaensis*

For increasing the frequency of crossover events in *S. toyocaensis*, the "stress" treatment described by Puk et al. [27] was modified. Cells were first grown in 50 ml R5 medium for 24 hr at 30°C, and then for an additional 24 hr at 37°C. For fragmentation, the mycelium was ultrasound treated as described. To obtain single colonies, protoplasts were prepared as described by Matsushima and Baltz [26].

Qualitative Determination of A47934 Production by Bioassay

A47934 production was determined by bioassays with *Bacillus subtilis* ATCC 6633 as the test organism [28], and cell supernatants of *S. toyocaensis* were grown in R5 medium.

HPLC-ESI-MS and -MS/MS

Investigations of the A47934 variants and precursors in the culture broths of the wild-type and mutant strains were performed via HPLC-ESI-MS and -MS/MS analyses. Culture broths were prepared by centrifugation and filtration to obtain particle-free samples. To optimize and facilitate the filtration of the supernatant, celite (Hyflo Super-Cel, Haeffner, Asperg, Germany) was added. In order to allow the detection of low-concentrated metabolites, particularly the biosynthetic intermediates of the wild-type cultures, several sample preparation procedures were tested. In all cases, an adsorption chromatography with AMBERLITE XAD16 and XAD1180 material was performed to remove large amounts of saccharose that had been added to the culture media. In subsequent steps, solid-phase extraction (bond elut C18, Varian, Darmstadt, Germany) as well as preparative HPLC were performed. The resulting fractions were analyzed by means of HPLC-ESI-MS and -MS/MS.

The HPLC-ESI-MS/MS system that was used consisted of a capillary-LC system (1100 series, Agilent Technologies Deutschland GmbH, Böblingen, Germany) coupled to a QTrap2000 with a TurboIonSpray source (Applied Biosystems, Darmstadt, Germany). Separations were performed on a Jupiter 4u Proteo 90A column system (main column, 150 × 1 mm; precolumn, 30 ×1 mm; Phenomenex, Aschaffenburg, Germany) with a flow rate of 50 μl min^{-1} in micro mode and the following gradient: t = 0 min, 5% B; t = 10 min, 20% B; t = 13 min, 50% B; t = 14 min, 100% B (solvent A: 0.1% HCOOH in water; solvent B: 0.1% HCOOH in acetonitrile). The injection volume was 5 μl. The TurboIonSpray source-dependent parameters were optimized for the flow rate of 50 μl min^{-1} to: CUR, 30; IS, 5500; nebulizer gas, 70; turbo gas, 70; TEM, 300. The compound-dependent parameters were optimized with different glycopeptide derivatives described previously [5, 6] to: DP, 30; EP, 12; CE, 10; Q3 entry barrier, 12. The EMS scans were carried out in positive mode, with a LIT scan rate of 1000 amu/s and dynamic fill time. The daughter ion scans had the following parameters: Q1 resolution unit; LIT scan rate, 1000 amu/s; fixed LIT fill time, 500 ms; CAD gas, high. In order to prevent secondary fragmentation, the most daughter ion scans were performed in time-delayed fragmentation (TDF) mode and with different collision energies.

Supplemental Data

Supplemental Data include all the PCR protocols, a table containing bacterial strains and plasmids, and a table containing the used oligonucleotides, and are available at http://www.chembiol.com/cgi/content/full/14/9/1078/DC1/.

ACKNOWLEDGMENTS

This research was supported by a grant of the European Union (COMBIG-TOP, LSHG-CT-2003-503491) and the Deutsche Forschungsgemeinschaft (DFG) (WO 485-1,2; SU 239/2) to W.W. and R.S. and by Schering AG to R.S. We thank Christian Rausch for the construction of the phylogenetic tree.

Received: July 2, 2007
Revised: August 10, 2007
Accepted: August 13, 2007
Published: September 21, 2007

REFERENCES

1. Nicolaou, K.C., Boddy, C.N., Bräse, S., and Winssinger, N. (1999). Chemistry, biology, and medicine of the glycopeptide antibiotics. Angew. Chem. Int. Ed. Engl. *38*, 2096–2152.
2. Williams, D.H., and Bardsley, B. (1999). The vancomycin group of antibiotics and the fight against resistant bacteria. Angew. Chem. Int. Ed. Engl. *38*, 1173–1193.
3. Wolter, F., Schoof, S., and Süssmuth, R.D. (2007). Synopsis of structural, biosynthetic, and chemical aspects of glycopeptide antibiotics. In Topics in Current Chemistry: Glycopeptide Chemistry, V. Wittman, ed. (Berlin/Heidelberg: Springer), pp. 143–185.
4. Pelzer, S., Reichert, W., Huppert, M., Heckmann, D., and Wohlleben, W. (1997). Cloning and analysis of a peptide synthetase gene of the balhimycin producer *Amycolatopsis mediterranei* DSM5908 and development of a gene disruption/replacement system. J. Biotechnol. *56*, 115–128.
5. Bischoff, D., Pelzer, S., Höltzel, A., Nicholson, G.J., Stockert, S., Wohlleben, W., Jung, G., and Süssmuth, R.D. (2001). The biosynthesis of vancomycin-type glycopeptide antibiotics-new insights into the cyclization steps. Angew. Chem. Int. Ed. Engl. *40*, 1693–1696.
6. Bischoff, D., Pelzer, S., Bister, B., Nicholson, G.J., Stockert, S., Schirle, M., Wohlleben, W., Jung, G., and Süssmuth, R.D. (2001). The biosynthesis of vancomycin-type glycopeptide antibiotics-the order of the cyclization steps. Angew. Chem. Int. Ed. Engl. *40*, 4688–4691.
7. Stegmann, E., Pelzer, S., Bischoff, D., Puk, O., Stockert, S., Butz, D., Zerbe, K., Robinson, J., Süssmuth, R.D., and Wohlleben, W. (2006). Genetic analysis of the balhimycin (vancomycin-type) oxygenase genes. J. Biotechnol. *124*, 640–653.
8. Süssmuth, R.D., Pelzer, S., Nicholson, G., Walk, T., Wohlleben, W., and Jung, G. (1999). New advances in the biosynthesis of glycopeptide antibiotics of the vancomycin type from *Amycolatopsis mediterranei*. Angew. Chem. Int. Ed. Engl. *38*, 1976–1979.
9. Süssmuth, R.D., and Wohlleben, W. (2004). The biosynthesis of glycopeptide antibiotics-a model for complex, non-ribosomally synthesized, peptidic secondary metabolites. Appl. Microbiol. Biotechnol. *63*, 344–350.
10. Hubbard, B.K., and Walsh, C.T. (2003). Vancomycin assembly: nature's way. Angew. Chem. Int. Ed. Engl. *42*, 730–765.
11. Bischoff, D., Bister, B., Bertazzo, M., Pfeifer, V., Stegmann, E., Nicholson, G.J., Keller, S., Pelzer, S., Wohlleben, W., and Süssmuth, R.D. (2005). The biosynthesis of vancomycin-type glycopeptide antibiotics-a model for oxidative side-chain cross-linking by oxygenases coupled to the action of peptide synthetases. ChemBioChem *6*, 267–272.
12. Zerbe, K., Woithe, K., Li, D.B., Vitali, F., Bigler, L., and Robinson, J.A. (2004). An oxidative phenol coupling reaction catalyzed by

 ©2007 Elsevier Ltd All rights reserved

OxyB, a cytochrome P450 from the vancomycin-producing microorganism. Angew. Chem. Int. Ed. Engl. *43*, 6709–6713.

13. Malabarba, A., Ferrari, P., Gallo, G.G., Kettenring, J., and Cavalleri, B. (1986). Teicoplanin, antibiotics from *Actinoplanes teichomyceticus* nov. sp. VII. Preparation and NMR characteristics of the aglycone of teicoplanin. J. Antibiot. (Tokyo) *39*, 1430–1442.
14. Boeck, L.D., and Mertz, F.P. (1986). A47934, a novel glycopeptide-aglycone antibiotic produced by a strain of *Streptomyces toyocaensis* taxonomy and fermentation studies. J. Antibiot. (Tokyo) *39*, 1533–1540.
15. Pootoolal, J., Thomas, M.G., Marshall, C.G., Neu, J.M., Hubbard, B.K., Walsh, C.T., and Wright, G.D. (2002). Assembling the glycopeptide antibiotic scaffold: the biosynthesis of A47934 from *Streptomyces toyocaensis* NRRL15009. Proc. Natl. Acad. Sci. USA *99*, 8962–8967.
16. Sosio, M., Kloosterman, H., Bianchi, A., de Vreugd, P., Dijkhuizen, L., and Donadio, S. (2004). Organization of the teicoplanin gene cluster in *Actinoplanes teichomyceticus*. Microbiology *150*, 95–102.
17. Donadio, S., Sosio, M., Stegmann, E., Weber, T., and Wohlleben, W. (2005). Comparative analysis and insights into the evolution of gene clusters for glycopeptide antibiotic biosynthesis. Mol. Genet. Genomics *274*, 40–50.
18. Stratmann, A., Toupet, C., Schilling, W., Traber, R., Oberer, L., and Schupp, T. (1999). Intermediates of rifamycin polyketide synthase produced by an *Amycolatopsis mediterranei* mutant with inactivated *rifF* gene. Microbiology *145*, 3365–3375.
19. Kammerer, B., Kahlich, R., Laufer, S., Li, S.M., Heide, L., and Gleiter, C.H. (2004). Mass spectrometric pathway monitoring of secondary metabolites: systematic analysis of culture extracts of *Streptomyces* species. Anal. Biochem. *335*, 17–29.
20. Bullock, W.O., Fernandez, J.M., and Short, J.M. (1987). XI1-Blue: a high-efficiency plasmid transforming recA *Escherichia coli* strain with β-galactosidase selection. Biotechniques *5*, 376–378.
21. Koutloubasi, M. (2004). Stammcharakterisierung von Streptomyces Lydicus ssp. Tanzanius NRRL 18036 und Screening nach dem Ganefromyciin-Biosynthese-Gencluster. Diploma thesis, Department of Microbiology/Biotechnology, Tübingen, Germany.
22. Bierman, M., Logan, R., O'Brien, K., Seno, E.T., Rao, R.N., and Schoner, B.E. (1992). Plasmid cloning vectors for the conjugal transfer of DNA from *Escherichia coli* to *Streptomyces* spp. Gene *116*, 43–49.
23. Sambrook, J., and Russel, D.W. (2001). The Condensed Protocols Molecular Cloning: A Laboratory Manual (Cold Spring Harbor, NY: Cold Spring Harbor Laboratory Press).
24. Sambrook, J., Fritsch, E.F., and Maniatis, T. (1989). Molecular Cloning: A Laboratory Manual (Cold Spring Harbor, NY: Cold Spring Harbor Laboratory Press).
25. Kieser, T., Bibb, J.M., Buttner, M.J., Chater, K.F., and Hopwood, D.A. (2000). Practical *Streptomyces* Genetics (Norwich, UK: John Innes Foundation).
26. Matsushima, P., and Baltz, R.H. (1996). A gene cloning system for '*Streptomyces toyocaensis*'. Microbiology *142*, 261–267.
27. Puk, O., Huber, P., Bischoff, D., Recktenwald, J., Jung, G., Süssmuth, R.D., van Pee, K.H., Wohlleben, W., and Pelzer, S. (2002). Glycopeptide biosynthesis in *Amycolatopsis mediterranei* DSM5908: function of a halogenase and a haloperoxidase/perhydrolase. Chem. Biol. *9*, 225–235.
28. Pelzer, S., Süssmuth, R., Heckmann, D., Recktenwald, J., Huber, P., Jung, G., and Wohlleben, W. (1999). Identification and analysis of the balhimycin biosynthetic gene cluster and its use for manipulating glycopeptide biosynthesis in *Amycolatopsis mediterranei* DSM5908. Antimicrob. Agents Chemother. *43*, 1565–1573.
29. Roepstorff, P., and Fohlman, J. (1984). Proposal for a common nomenclature for sequence ions in mass spectra of peptides. Biomed. Mass Spectrom. *11*, 601.